Journal of Alloys and Compounds 502 (2010) 495–502

Contents lists available at ScienceDirect

Journal of Alloys and Compounds

journal homepage: www.elsevier.com/locate/jallcom

A comparative study of the wear behavior of as-cast and hot extruded ZE41A magnesium alloy

S. Anbu selvan*, S. Ramanathan

Department of Manufacturing Engineering, Annamalai University, Annamalai Nagar, Chidambaram 608002, Tamil Nadu, India

ARTICLE INFO

Article history:
Received 26 November 2009
Received in revised form 27 April 2010
Accepted 28 April 2010
Available online 5 May 2010

Keywords:
Dry sliding wear
ZE41A magnesium alloy
Effects of extrusion
Wear mechanisms
Comparison of wear behavior

ABSTRACT

Dry sliding wear tests were performed on as-cast and hot extruded ZE41A magnesium alloy using pin-on-disc (EN32 steel) configuration. Wear rates were measured in an applied load range of 30–150 N, sliding velocity range of 0.5–2.5 m/s and at a constant sliding distance of 1500 m. Microstructures of worn surfaces were characterized by scanning electron microscope (SEM) and energy dispersive spectrometer (EDS). Wear maps were drawn. The dominant wear mechanisms in each wear regime were identified and classified in wear mechanism maps. Extruded alloy showed better wear resistance and exhibited good tribological properties than as-cast alloy due to grain refinement, decrease in porosity, strengthening and hardening of the material.

1. Introduction

Magnesium alloys are attractive materials for use in aircraft structures, due to the low densities, good casting properties and high specific buckling resistance [1]. These alloys maintain significant usage in certain machine housings, aerospace, automotive, space, and nuclear applications [2]. For most of the applications the components require a modification to the surface as magnesium alloys exhibit a poor corrosion and wear resistance [3]. However, porosity may easily form in as-cast magnesium alloys. Thus, it always suffers from the challenge in meeting the requirements of strength, ductility, fatigue and creep resistance. In order to improve these properties, forming process has been adapted to produce components because one of the most salient advantages of this forming technology is to decrease or eliminate porosity [4]. Severe plastic deformation techniques have been used successfully to process ultrafine-grained microstructures in numerous metals [5]. It is tempting to use the refined grain structure of the magnesium alloy in order to enhance their mechanical properties including ductility and strength [6]. One of the most important advantages for today's technology is that magnesium can be easily recycled [3]. Recycling of magnesium alloys yielded fine grained specimen with considerable improvement in hardness and strength. The superior mechanical properties of these alloys suggest their suitability in friction and wear applications [7]. To improve mechanical properties, forming process has been adapted to produce components with a unique microstructure with small spherical primary particles uniformly distributed in the matrix, which is essentially different from those produced by using conventional casting techniques [8,9]. However, as a structural material, it is expected that a sliding motion between components is inevitable in some certain applications. In addition, sliding wear is also an important consideration in material processing by rolling, extrusion, forging, etc., from the point of view of understanding the changes in the deformation microstructure at the work-tool interface [10]. Therefore, the sliding wear behavior of magnesium alloys, produced by whatever processing route, is an important scientific focus and it is worthy of being paid much attention. Also in view of its potential applications in helicopter rotor gear box and engine components, it is essential to understand the tribological behavior of the alloy. In the 1970s, it was first reported that the magnesium alloy with high zinc revealed good creep resistance and good die castability [11]. In recent years, new magnesium alloys have been proposed incorporating rare-earth elements to improve their characteristics for different applications [12]. Rare earth (RE) has many merits, such as purifying alloy melt, modifying castability, refining the microstructure, improving the mechanical properties and anti-oxidization properties. Therefore, RE has been used in magnesium alloys for many years, such as Mg–Zn–RE–Zr [13]. Zirconium addition to rare-earth containing magnesium alloys has been shown to improve the mechanical properties due to grain refinement [14].

Published work on the wear behavior of magnesium alloy is quite limited. Bala Srinivasan et al. [15] studied the dry sliding wear behavior of conventional and recycled AZ91D magnesium alloy

* Corresponding author. Tel.: +91 9865387907; fax: +91 4144239734.
E-mail address: anbushankari@yahoo.co.in (S. Anbu selvan).

0925-8388/$ – see front matter © 2010 Elsevier B.V. All rights reserved.
doi:10.1016/j.jallcom.2010.04.205

using ball-on-disc tests under three different loads at a constant sliding velocity. They concluded that the recycled alloy showed better wear resistance when compared to the conventional alloy. They assessed that higher hardness and relatively higher volume fraction of β-phase with a denser distribution near the surface in recycled alloy were the reasons for improved wear behavior. Mondal and Kumar [16] studied the dry sliding wear behavior of AE42 magnesium alloy and its composites using pin-on-disc tests under four different loads at a constant sliding velocity and sliding distance. They observed that the wear rate of composites was lower than the alloy. Habibnejad-Korayem et al. [17] investigated the wear behavior of pure Mg and AZ31 Mg alloy and their composites reinforced with 2 wt.% Al_2O_3 nano-particles. The wear tests were conducted using pin-on-disc configuration with various applied stress, sliding speed and sliding distance. They concluded that the composites showed better wear resistance than pure magnesium and its alloy because of grain refinement, higher hardness and higher load bearing capacity. Guo et al. [18] reported the tribological behavior of plasma electrolytic oxidation coating (PEO) on AM60B magnesium alloy with oil lubrication at elevated temperatures. The tribological performance of the PEO coatings and uncoated magnesium alloys at different loads and elevated temperatures was comparatively investigated. They observed that the PEO coating exhibited significantly higher wear resistance when compared with Mg alloy due to the higher hardness and micro-pores structure feature of the PEO coating. Ding et al. [19] studied the wear behavior of AZ31 magnesium alloy and its composites with SiC_p using gas tungsten arc (GTA) surface modification process. They concluded that the microhardness and wear resistance of composites were superior to that of as-received AZ31 magnesium alloy. Chen et al. [20] investigated the friction and wear properties of thixoformed (TF) and permanent mould cast (PMC) AZ91D magnesium alloys under dry reciprocating sliding conditions using ball-on-disk method. The results indicated that the wear resistance of the TF alloy was significantly superior to that of the PMC alloy. Blau and Walukas [21] investigated the sliding friction and wear of magnesium alloy AZ91D produced by die-cast (DC) and Thixomolded (ThM) in both unidirectional and reciprocating sliding motion, using stainless steel type 440C as counterface. Test results indicated that the average wear rate of ThM alloys in reciprocating sliding was approximately 25% lower than that for DC alloys. El-Morsy [22] investigated the wear behavior of extruded magnesium alloy AZ61 during dry sliding. The experiments were performed using a pin-on-ring type wear apparatus against a stainless steel counterface. He observed that the sliding wear behavior can be classified in to two main wear regimes, mild wear regime and a severe wear regime. An et al. [23] investigated the dry sliding wear behavior of as-cast magnesium alloys $Mg_{97}Zn_1Y_2$ and AZ91 using a pin-on-disc configuration. They observed five wear mechanisms namely abrasion, oxidation, delamination, thermal softening and melting. Also, they reported that $Mg_{97}Zn_1Y_2$ magnesium alloy exhibited good wear resistance than AZ91 magnesium alloy. Hiratsuka et al. [24] investigated the dry sliding wear of pure magnesium against an alumina counterface using a pin-on-disc apparatus. They observed two different wear mechanisms depending on the testing environment. Magnesium exhibited an oxidational wear mechanism when tested in air. When the wear tests under the same load and velocity conditions were repeated in vacuum (2.5×10^{-4} Pa), magnesium showed metallic wear. Aung et al. [25] investigated the wear behavior of AZ91D alloy at low sliding speeds under dry sliding conditions using pin-on-disc configuration. The wear rates were measured under a constant load at two different sliding distances. They observed three wear mechanisms such as abrasion, oxidation and delamination at lower sliding speeds. Chen and Alpas [10] reported the dry sliding wear map for AZ91D magnesium alloy against AISI 52100 steel counterface. They discussed the different wear regimes, summarized a wear mechanism map, and developed an empirical contact surface temperature model to predict the critical surface temperature at the onset of severe wear. Zhang and Alpas [26] constructed a wear map for a wrought aluminium alloy 6061 sliding against AISI 52100 steel. It was shown that mild to severe wear transition that occurs at a certain combination of load, velocity and sliding distance was controlled by a surface temperature criterion which coincided with the threshold temperature at which thermally activated processes, such as dynamic recrystallization initiated. The wear mechanisms identified on the wear map included delamination of oxidized layers, delamination of subsurface layers, severe deformation induced wear and seizure. The same mechanisms were observed in cast aluminium alloys [27].

The results of literature survey indicate that no attempts have been made to investigate the effects of extrusion on the wear behavior of magnesium alloy. In the present work, dry sliding wear behavior of hot extruded ZE41A magnesium alloy is compared with as-cast magnesium alloy using a pin-on-disc type wear apparatus against an EN32 steel counterface.

Table 1
Mechanical properties of as-cast and extruded ZE41A magnesium alloy.

Materials	Grain size (μm)	Microhardness (HV)	UTS (MPa)	Ductility (% EL)
As-cast alloy	78.2 ± 5	65.1 ± 0.3	206.1 ± 4	4.6 ± 0.2
Extruded alloy	41.3 ± 4	74.5 ± 0.6	310.3 ± 2	3.2 ± 0.3

2. Experimental details

2.1. Materials

The material used in this work was ZE41A magnesium alloy with the following composition in weight percent: 3.85%Zn, 1.27%Ce, 0.53%Zr, 0.002%Cu, 0.006%Al, 0.008%Mn, 0.004%Fe, 0.003%Si, 0.002%Ni and the balance Mg. The as-cast material was machined into 31 mm diameter and 50 mm length for hot extrusion. The small ingots were then extruded at 300 °C with a rate of 4 m/min to give solid bars with diameters of 17 mm corresponding to reduction ratio in the area of 70%. The initial microstructure of as-cast and extruded ZE41A magnesium alloy is shown in Fig. 1(a) and (b). Also the mechanical properties of as-cast and extruded alloy are shown in Table 1.

2.2. Sliding wear test

Dry sliding wear tests were performed on a tribometer testing machine of pin-on-disc type wear apparatus against EN32 steel counterface. Wear test samples in the form of cylindrical pin with 30 mm in length and 6 mm in diameter were machined from as-cast and extruded specimens. Contact surfaces were prepared by grinding against 600 – grid silicon carbide paper and cleaned ultrasonically in a methanol solution. The counterface was EN32 steel disc (HRC65) of 160 mm diameter and 8 mm width having surface roughness of 0.02 μm on which the test specimen slide. The tests were carried out in an applied load range of 30–150 N and a sliding velocity range of 0.5–2.5 m/s. The constant sliding distance was about 1500 m. The mass losses were calculated from the differences in weight of specimens measured before and after the sliding test (after removing any loose debris) using a precision balance (0.001 g). Volumetric wear rate was calculated by dividing the volumetric wear loss by sliding distance. Each test was carried out twice in order to check the reproducibility and average of two tests was taken to determine the wear rate. Microstructural investigations on the worn surfaces were undertaken using a scanning electron microscope (SEM) (Model JSM 5610 LV) equipped with an energy dispersive spectrum (EDS).

3. Results and discussion

3.1. Wear behavior

The volumetric wear rates of as-cast and extruded ZE41A magnesium alloy are plotted against applied load for the tests conducted at a constant sliding speed of 0.5, 1.0, 1.5, 2.0 and 2.5 m/s in Fig. 2. At all sliding speeds, the wear rate is increased with increasing applied load for both alloys. For as-cast alloy large changes in slope of wear rates occurred at 60 N. The slope changes coincided

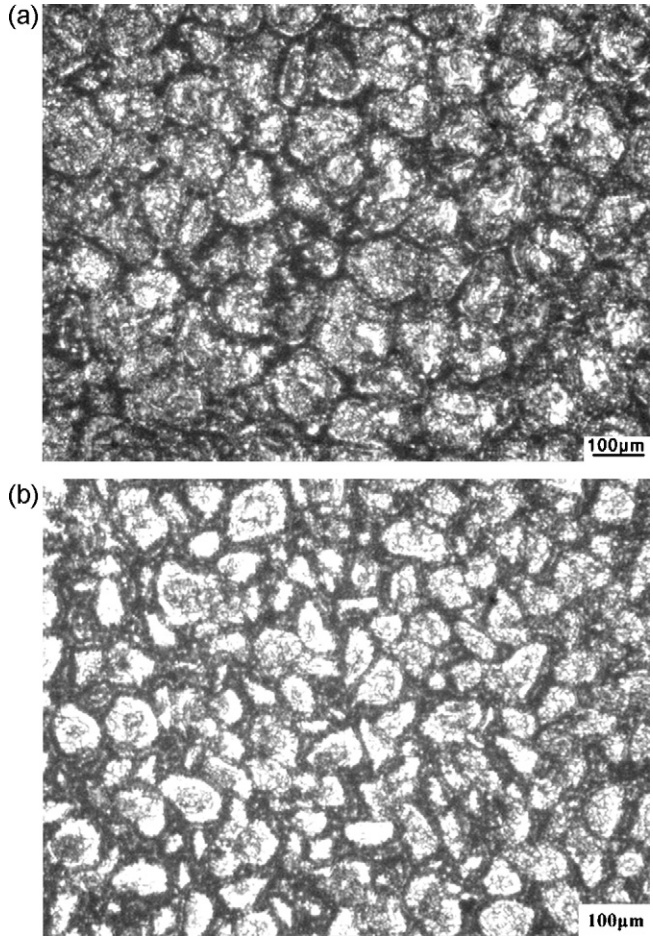

Fig. 1. Initial microstructure of ZE41A magnesium alloy (a) as-cast alloy; (b) extruded alloy.

with the transition from mild to severe wear [10]. For extruded alloy, large changes in slope of wear rates occurred at 90 N. These indicate that mild wear maintains up to 60 N for as-cast alloy and 90 N for extruded alloy. The effect of sliding velocity on the volumetric wear rates at a constant applied load of 30, 60, 90, 120 and 150 N for as-cast and extruded alloy is shown in Fig. 3. At all applied loads, the wear rate is increased with increasing sliding velocity

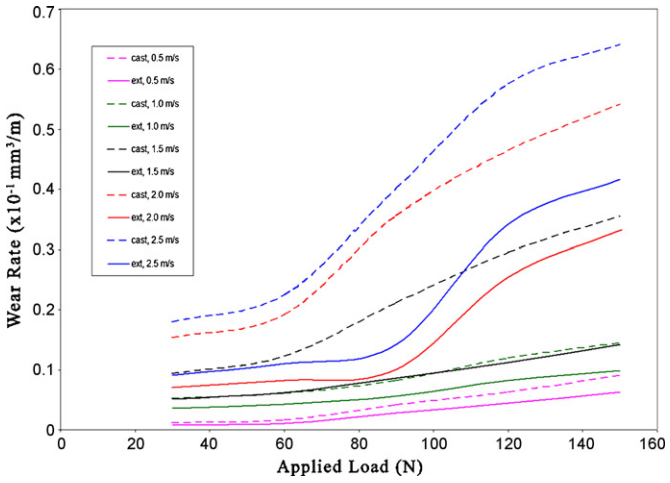

Fig. 2. Effect of applied load on the wear rate of as-cast and extruded ZE41A magnesium alloy at different sliding velocities.

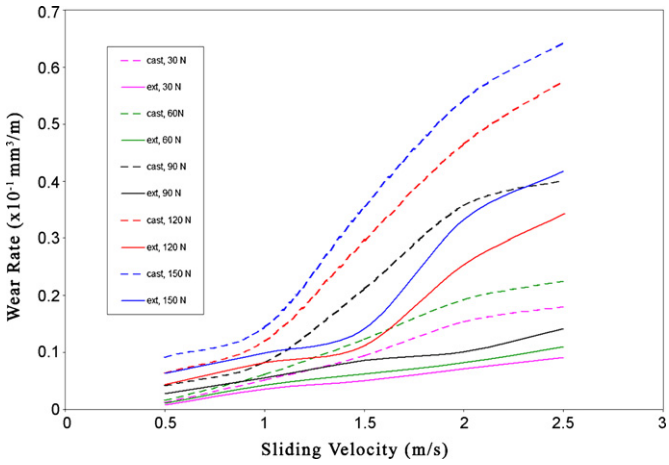

Fig. 3. Effect of sliding velocity on the wear rate of as-cast and extruded ZE41A magnesium alloy at different applied loads.

for both alloys. Large changes in slope of wear rates occurred at 1.0 m/s for as-cast alloy and 1.5 m/s for extruded alloy. These indicate that mild wear maintains up to 1.0 m/s for as-cast alloy and 1.5 m/s for extruded alloy. From Figs. 2 and 3, it is observed that the extruded alloy has lower wear rate than as-cast alloy at all applied load and sliding velocity conditions. This is achieved by grain refinement, less porosity, strengthening and hardening of the material by hot extrusion. This is well agreed with Lin et al. [28], Chandrasekaran and John [29] and El-Morsy et al. [30]. According to the well known Hall–Petch relationship, the refinement in grain size will be resulted in the strengthening or hardening of the materials, thereby in accordance with Archard's law [31]:

$$\frac{V}{L} = \frac{KW}{H}$$

where V is the volume of wear; L the sliding distance; W the normal load; H the hardness of softer one in two contacting materials (ZE41A in the present work); and K is the wear coefficient. From Archard's law, it is observed that the wear volume decreases with an increase in pin hardness. In Table 1, it is clearly mentioned that the strength and hardness of extruded alloy is higher than as-cast alloy. Also the grain size of ZE41A magnesium alloy is reduced from 78.2 to 41.3 μm due to extrusion. Therefore, the wear resistance of extruded ZE41A magnesium alloy is improved by the decrease in grain size, increase in strength and hardness. Similar findings were reported by Habibnejad-Korayem et al. [17], Chena et al. [32], and Ding et al. [33].

3.2. Wear mechanisms

Scanning electron microscopic examinations of both as-cast and extruded worn pin surfaces identified five different wear mechanisms operating under various sliding conditions. They are abrasion, oxidation, delamination, plastic deformation and melting. In the following sections, the observed wear mechanisms are discussed in relation to the sliding conditions and wear rates so as to better understand the tribological characteristics and identify the useful range of these magnesium alloys.

3.2.1. Abrasion

Abrasion wear occurred in the as-cast worn surfaces at 30 N and 0.5 m/s also in the extruded worn surfaces at 60 N and 0.5 m/s as shown in Fig. 4(a) and (b), respectively. Numerous grooves and scratch marks, mostly parallel to the sliding direction, are evident on all the worn pins. Such features are characteristics of abrasion, in which hard particles in between the contacting surfaces, plough

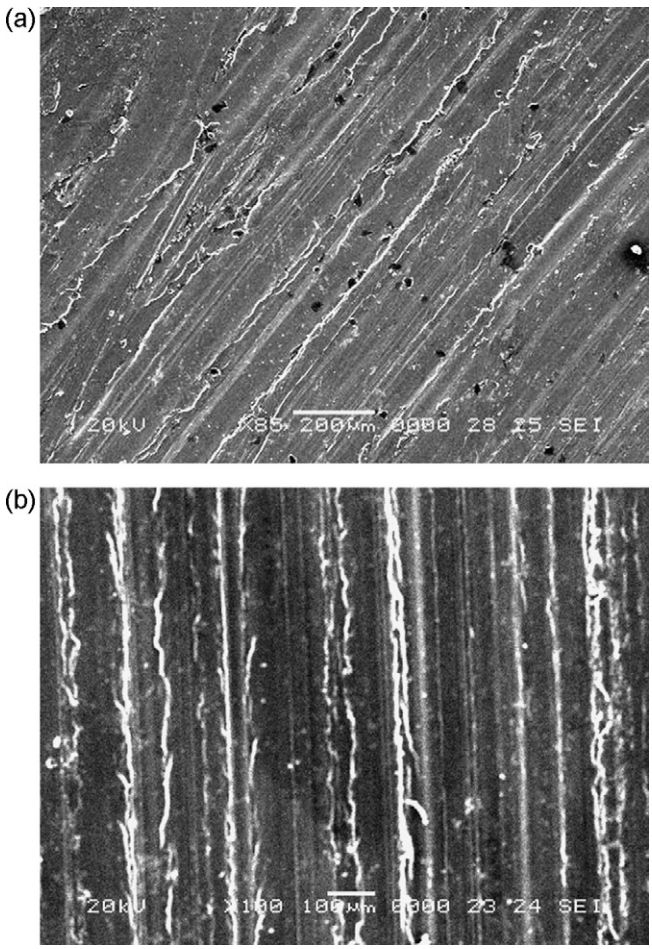

Fig. 4. SEM micrographs showing grooves and scratch marks on the pin surfaces, indicating abrasion (a) as-cast alloy at 30 N and 0.5 m/s; (b) extruded alloy at 60 N and 0.5 m/s.

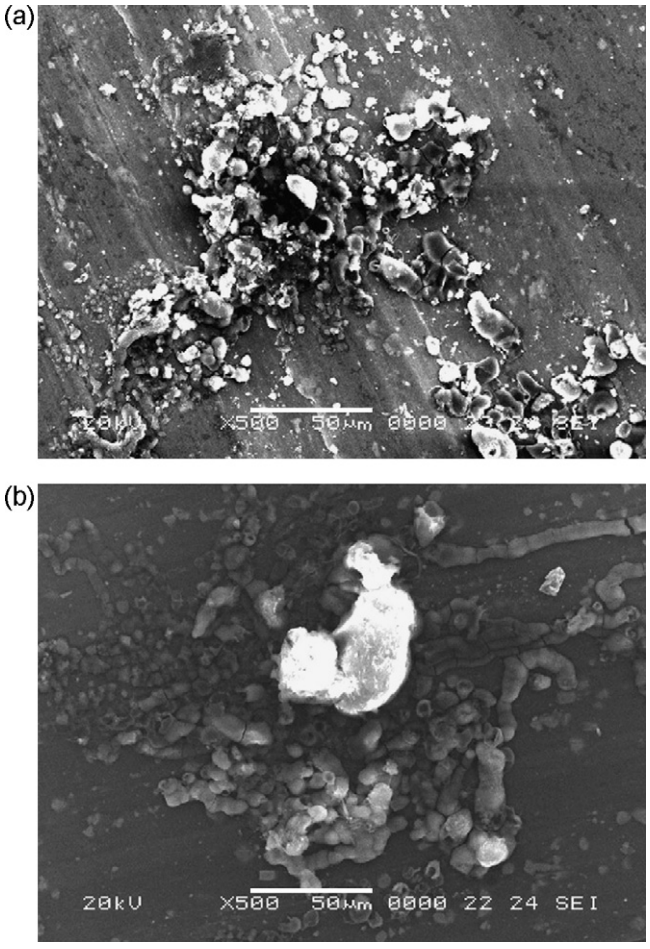

Fig. 5. SEM micrographs showing oxidation (a) as-cast alloy at 30 N and 1.0 m/s; (b) extruded alloy at 60 N and 1.0 m/s.

or cut into the pin, causing wear by the removal of small fragments [22]. This suggests that abrasion took place primarily via ploughing, in which material is displaced on either side of the abrasion groove without being removed, or wedge forming, where tiny wedge-shaped fragments are worn only during the initial contact with an abrasive particle. This is well agreed with earlier investigation [34].

3.2.2. Oxidation

Fig. 5(a) shows the SEM image of oxidation wear for as-cast samples at 30 N and 1.0 m/s. Fig. 5(b) shows the SEM image of oxidation wear for extruded samples at 60 N and 1.0 m/s. Under SEM, the dark surfaces are found to be covered extensively by a thin layer of fine particles as shown in Fig. 5. The EDS analysis (Fig. 6) indicates the presence of a strong oxygen peak in addition to the magnesium peak. These characteristics are indicative of oxidative wear, in which frictional heating during sliding causes oxidation of the surface, with wear occurring through the removal of oxide fragments. Over repeated sliding, oxide wear debris fills out the valleys on the pin surface, and becomes compacted in to a protective layer. So metallic contact is prevented and minimum wear rates are occurred [35].

3.2.3. Delamination

Fig. 7(a) shows the SEM image of delamination wear for as-cast samples at 60 N and 1.0 m/s. Fig. 7(b) shows the SEM image of delamination wear for extruded samples at 90 N and 1.0 m/s. As the applied load is increased in the mild wear regime, a gradual

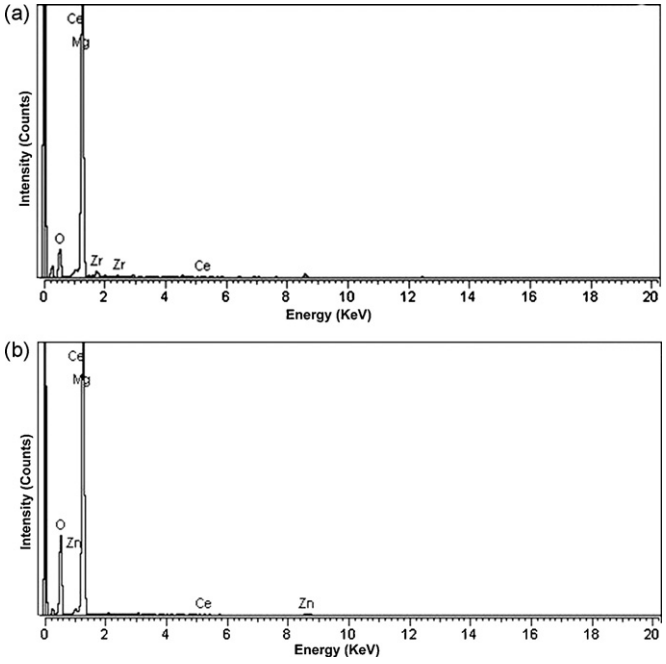

Fig. 6. EDS analysis showing strong oxygen peaks, indicating oxidation of worn surfaces (a) as-cast alloy at 30 N and 1.0 m/s; (b) extruded alloy at 60 N and 1.0 m/s.

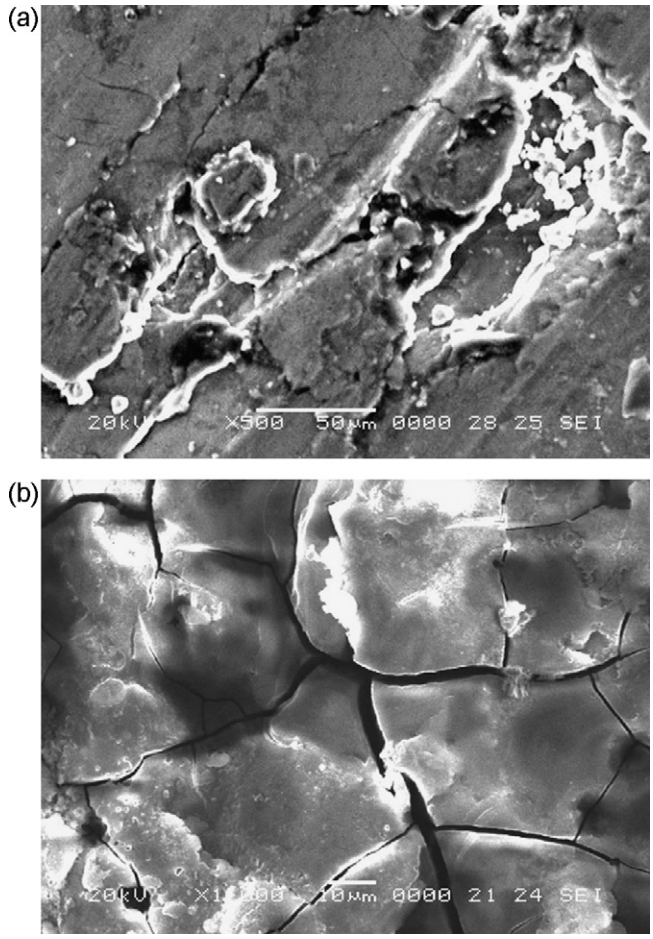

Fig. 7. SEM micrographs showing series of cracks roughly perpendicular to the sliding direction on the pin surface, indicating delamination (a) as-cast alloy at 60 N and 1.0 m/s; (b) extruded alloy at 90 N and 1.0 m/s.

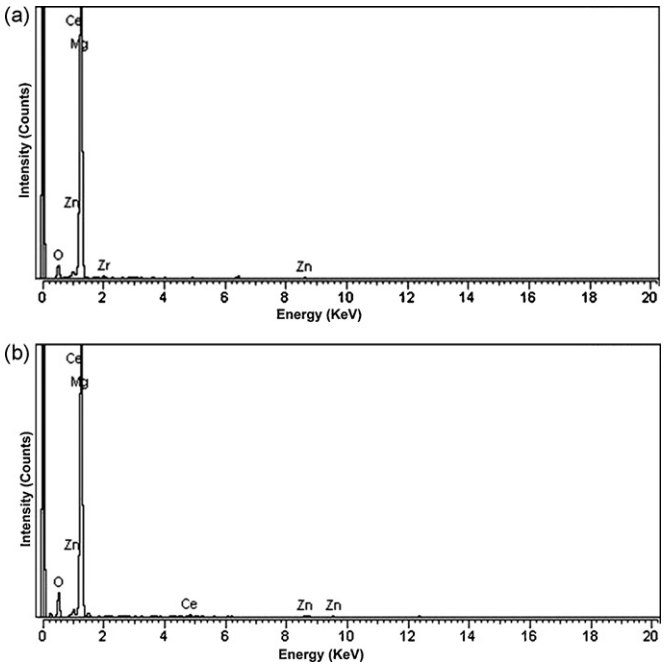

Fig. 8. EDS analysis showing the presence of an oxygen peak of low intensity, indicating the surface is slightly oxidized (a) as-cast alloy at 60 N and 1.0 m/s; (b) extruded alloy at 90 N and 1.0 m/s.

transition in the wear behavior of the alloy occurred from an oxidational wear to a delamination wear [10]. The presence of an oxygen peak of low intensity in the EDS spectrum of Fig. 8 implied that the surface is slightly oxidized when the freshly produced surfaces of the detached particles became in contact with the air. In delamination wear, short cracks occur roughly perpendicular to the sliding direction. The intersection of these cracks results in the detachment of sheet-like wear particles. In delamination wear the subsurface cracks, which may either exist earlier or get nucleated due to the stresses, propagate during the course of wear. When such subsurface cracks join the wear surface, delamination is the dominant wear mechanism [36]. Similar kind of observations was made by Sharma et al. [37].

3.2.4. Plastic deformation

Fig. 9(a) shows the plastic deformation layer on the worn surface of as-cast samples tested at 90 N and 1.5 m/s. Fig. 9(b) shows the plastic deformation layer on the worn surface of extruded samples tested at 120 N and 1.5 m/s. Venkataraman and Sundararajan [38] suggested that the transition from delamination to plastic deformation occurred at higher loads and speeds. At higher applied load and sliding velocity conditions, extensive surface damage as a result of plastic deformation of the material layers adjacent to the contact surface is the main wear mechanism. The severely deformed material layers extruded along the sliding direction and out of the contact surface of the sample [10]. It is known that the temperature at the contact surface between steel counterface and test specimen during these conditions could reach high temperatures. The transi-

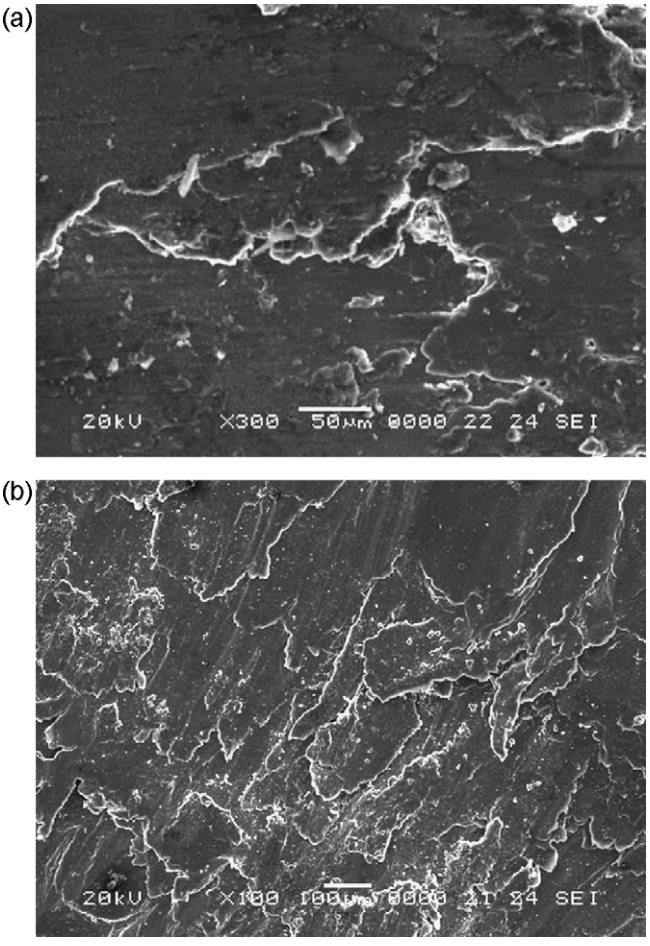

Fig. 9. SEM micrographs showing plastic deformation of worn surfaces (a) as-cast alloy at 90 N and 1.5 m/s; (b) extruded alloy at 120 N and 1.5 m/s.

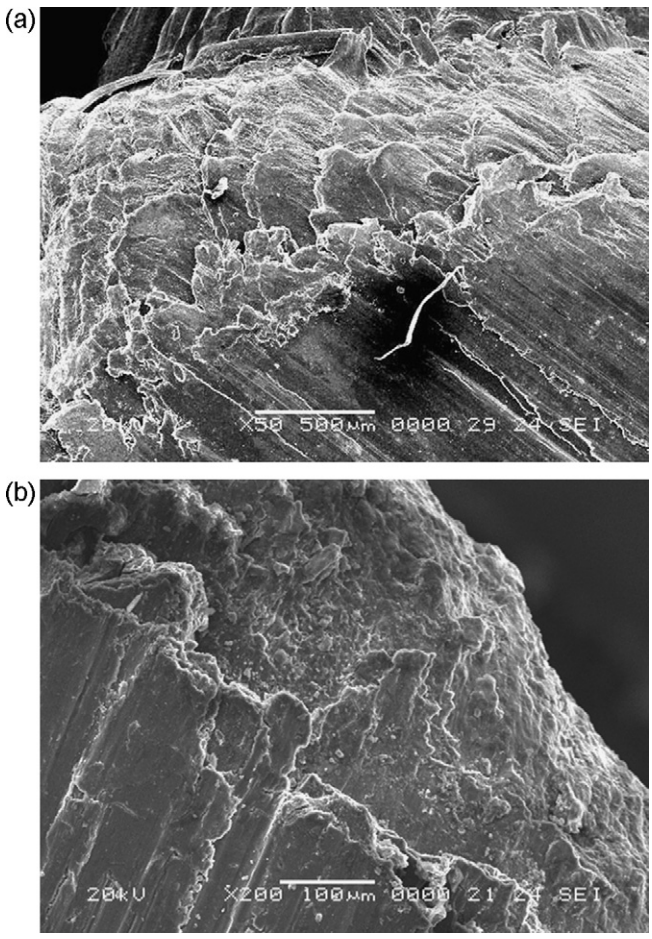

Fig. 10. SEM micrographs showing surface melting of worn surfaces (a) as-cast alloy at 120 N and 2.0 m/s; (b) extruded alloy at 150 N and 2.0 m/s.

tion between mild to severe wear was accompanied by a significant increase in the roughness of worn surface of samples [26]. The increase in applied load and sliding velocity resulted in an increase in plastic deformation, which resulted in high level of structural disruption and extensive damage for the material. As the temperature increases the yield strength of both as-cast and extruded alloy decreases sharply and gets softened. As a result, they become prone to easy plastic deformation and spread out of the contact surface in the direction of sliding as well as by moving side ways [39].

3.2.5. Melting

Fig. 10(a) shows the SEM image of surface melting on the worn surface of as-cast samples tested at 120 N and 2.0 m/s. Fig. 10(b) shows the SEM image of surface melting on the worn surface of extruded samples tested at 150 N and 2.0 m/s. When the sliding speed and applied load reaches certain critical thresholds, flash temperatures at contacting asperities could exceed the melting point of the alloy, thus increasing bulk temperature and causing gradual softening of both as-cast and extruded alloy. Continued sliding or increases in speed and load would raise temperatures further, leading to melting and rapid increase in wear rate [35]. Chen and Alpas [10] reported that, during the wear tests at the highest applied loads, i.e. above 140 N, there was evidence that the local temperature of the contact surfaces exceeded the melting temperature of the alloy results friction-induced surface melting. The molten material spread out of the contact surface in the sliding direction as well as by moving sideways. During the sliding wear, the solidified material formed thin layers. The new layers were continuously generated over the previously formed layers as the previously molten material extruded out of the contact surface.

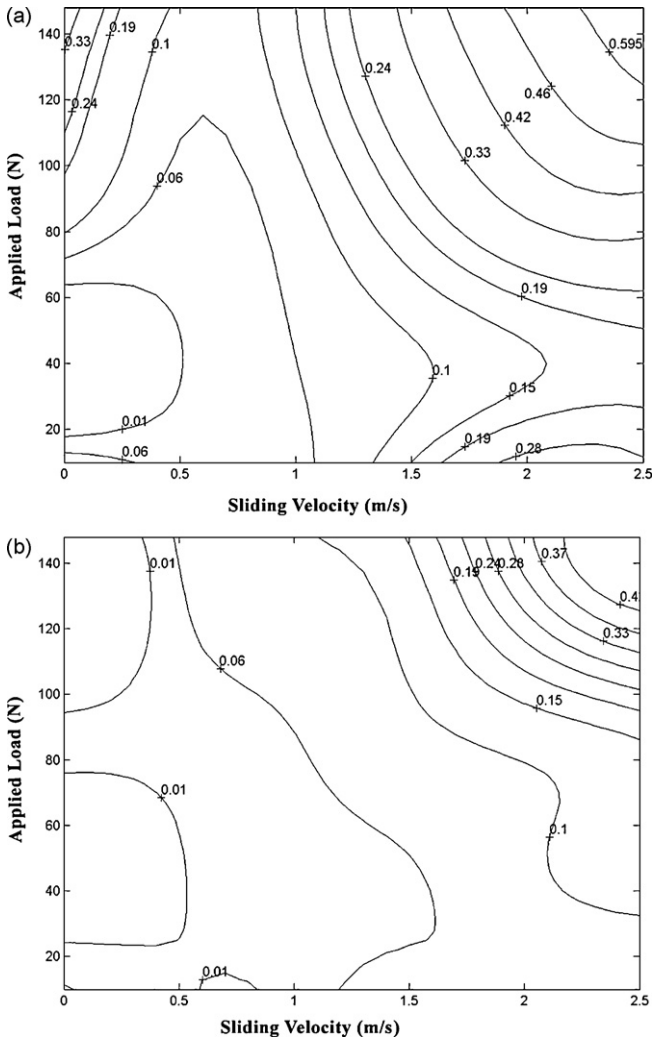

Fig. 11. Wear rate maps of ZE41A magnesium alloy (a) as-cast alloy; (b) extruded alloy.

3.3. Wear rate map

Wear rate maps are necessary to understand the wear characteristics of a given material over a range of operating conditions. Once the maps are generated, they allow subsequent analysis in terms of wear transition maps and wear mechanism maps [40]. Fig. 11(a) and (b) shows the wear rate map of as-cast and extruded ZE41A magnesium alloy for various dry sliding conditions, respectively. These contour wear rate maps have been constructed on applied load versus sliding velocity axis using MAT LAB software and wear rate data. Each contour represents the wear rate for different applied load and sliding velocity conditions. The wear rate data are in $mm^3/m \times 10^{-1}$. For both as-cast and extruded alloys, the wear rate is minimum at lower applied load and sliding velocity conditions and it is maximum at higher applied load and sliding velocity conditions.

3.4. Wear mechanism map

The wear mechanism map defines regions where the material behavior is nearly the same. These regions are separated by transition lines or bands which are functions of two or more param-

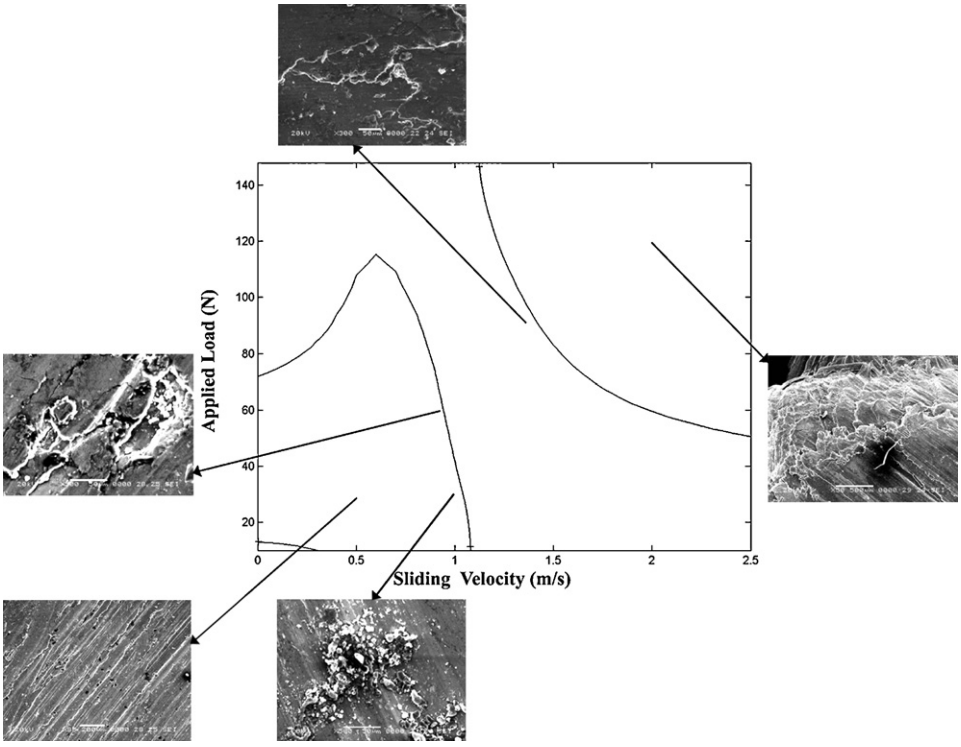

Fig. 12. Wear mechanism map of as-cast ZE41A magnesium alloy sliding against EN32 steel counterface.

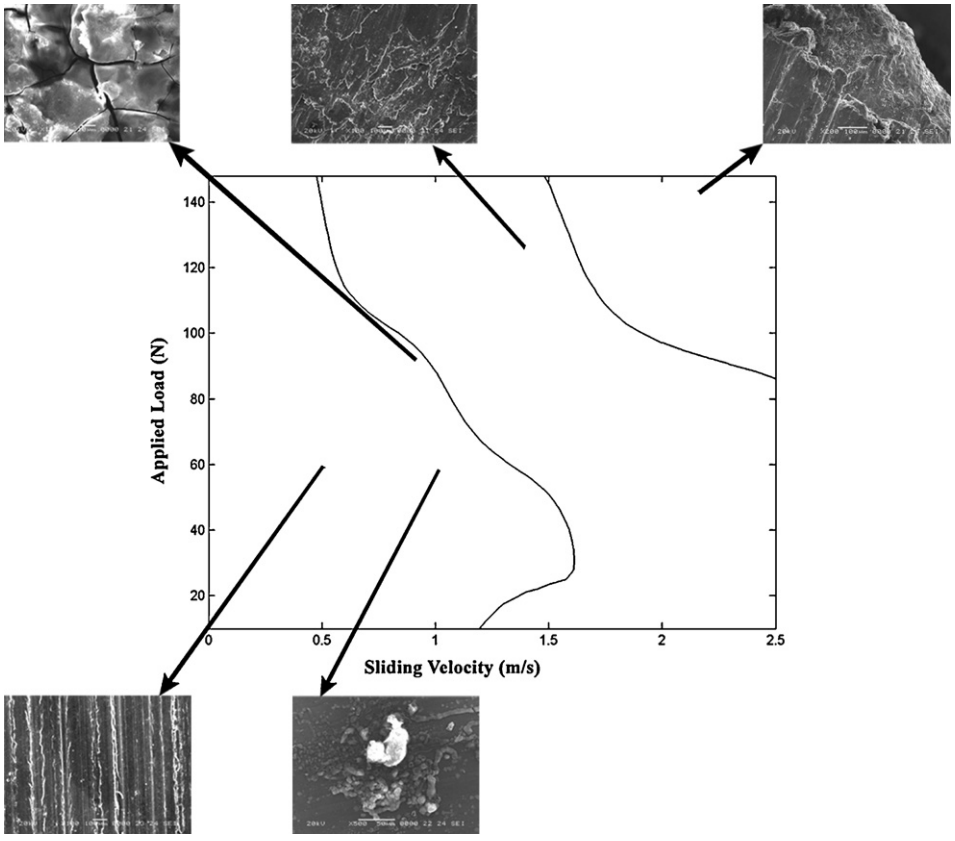

Fig. 13. Wear mechanism map of extruded ZE41A magnesium alloy sliding against EN32 steel counterface.

eters. Once the behavior of a given pair of materials is mapped, the maps can be used to understand the mechanisms that control wear, as material selection guides, as well as design guides for different engineering applications [41]. By examining the contour maps (lines of constant wear rate), lines of equal spacing and lack of curvature usually indicate the same dominant mechanism. Valleys and plateaus usually suggest some change in the wear mode. In this way, regions with potentially different wear mechanism can be identified. Wear mechanism maps summarizing data and models for wear, showing how the mechanisms interface, and allowing the dominant wear mechanisms for any given set of conditions to be identified. Wear mechanism map could be developed to explore this much broader pattern of wear behavior [40]. Zhang and Alpas [26] suggested that wear mechanism map can be a useful tool to predict the conditions under which a tribosystem can operate safely. Wear mechanism map can also serve as a guide line to select wear resistant materials and suitable counterfaces for them. Figs. 12 and 13 show the wear mechanism map for as-cast and extruded ZE41A magnesium alloy, respectively. Three wear regimes are achieved as mild wear, severe wear and ultra severe wear for both as-cast and extruded alloys. The transition boundary between mild to severe wear and severe to ultra severe wear is not based on a specific wear rate criterion [10]. In mild wear regime, the wear occurs by abrasion, oxidation and delamination of the bulk material. These wear mechanisms are dominant in the mild wear regime. For practical applications, this regime can be regarded as "safe" operation regime since the wear rates are typically low and wear proceeds under steady-state condition [26]. Plastic deformation induced wear is the dominant wear mechanism in the severe wear regime. Increase in applied load and sliding velocity cause local temperature rises at contact surfaces of the alloy results gross plastic deformation. The transition from mild to severe wear is controlled by applied load and sliding velocity. Surface melting is the dominant wear mechanism in the ultra severe wear regime. Further increase in applied load and sliding velocity cause high contact temperatures between pin and disc and also increase in frictional heat which results surface melting. The transition from severe wear to ultra severe wear is also controlled by applied load and sliding velocity. Comparing the wear mechanism map for as-cast and extruded ZE41A magnesium alloy, it is observed that there is an increase in mild wear regime and decrease in severe wear regime for extruded material. It means the safe operating regime for extruded ZE41A magnesium alloy is higher than as-cast magnesium alloy.

4. Conclusions

From the study reported above, the following conclusions can be drawn.

- The wear rate increases with an increase in applied load and sliding velocity for both as-cast and extruded ZE41A magnesium alloy.
- The extruded alloy showed better wear resistance compared with as-cast alloy. Wear surfaces revealed that the sliding wear behavior of as-cast and extruded ZE41A magnesium alloy can be classified in to three wear regimes, namely mild wear, severe wear and ultra severe wear when characterized by scanning electron microscope.
- The dominant wear mechanisms in each regime were identified and summarized in the wear mechanism map.
- Increase in mild wear regime was found in extruded alloy as compared with as-cast alloy. Therefore, the safe operating regime for extruded ZE41A magnesium alloy is higher than as-cast alloy.
- The good tribological property was achieved in extruded ZE41A magnesium alloy due to grain refinement, decrease in porosity, strengthening and hardening of the material.

Acknowledgements

The authors would wish to thank Hindustan Aeronautic Limited (HAL), Bangalore, India for providing material and technical assistance. The invaluable contribution of Professor P.G. Venkatakrishnan, Government college of Engineering, Salem, India in conducting the wear test is gratefully acknowledged.

References

[1] S. Guldberg, H. Westengen, D.L. Albright, SAE Trans. (1991) 813–816 (Sec. 5).
[2] K.R. Baldwin, D.J. Bray, G.D. Howard, R.W. Gardiner, Mater. Sci. Technol. 12 (1996) 937–943.
[3] J.E. Gray, B. Luan, J. Alloys Compd. 336 (2002) 88–113.
[4] M.C. Flemings, Metall. Trans. A 22 (1991) 957–981.
[5] C. Xu, M. Furukawa, Z. Horita, T.G. Langdon, J. Alloys Compd. 378 (2004) 27–34.
[6] H. Takamura, T. Miyashita, A. Kamegawa, M. Okada, J. Alloys Compd. 356–357 (2003) 804–808.
[7] M. Shanthi, C.Y.H. Lim, L. Lu, Tribol. Int. 40 (2007) 335–338.
[8] F. Czerwinski, A. Zielinska-Lipiec, P.J. Pinet, J. Overbeeke, Acta Mater. 49 (2001) 1225–1235.
[9] F. Czerwinski, A. Zielinska-Lipiec, Acta Mater. 51 (2003) 3319–3332.
[10] H. Chen, A.T. Alpas, Wear 246 (2000) 106–116.
[11] J.F. King, Mg Alloys and their Applications, Wolfsburg, Germany, April 1998, pp. 37–47.
[12] Q. Li, Q.D. Wang, Y.X. Wang, X.Q. Zeng, W.J. Ding, J. Alloys Compd. 427 (2007) 115–123.
[13] L.Y. Wei, G.L. Dunlop, H. Westengen, Metall. Mater. Trans. A 26 (1995) 1947–1955.
[14] G. Ben-Hamu, D. Eliezer, K.S. Shin, S. Cohen, J. Alloys Compd. 431 (2007) 269–276.
[15] P. Bala Srinivasan, C. Blawert, W. Dietzel, Mater. Charact. 60 (2009) 843–847.
[16] A.K. Mondal, S. Kumar, Wear 267 (2009) 458–466.
[17] M. Habibnejad-Korayem, R. Mahmudi, H.M. Ghasemi, W.J. Poole, Wear 268 (2010) 405–412.
[18] J. Guo, L. Wang, J. Liang, Q. Xue, F. Yan, J. Alloys Compd. 481 (2009) 903–909.
[19] W. Ding, H. Jiang, X. Zeng, D. Li, S. Yao, J. Alloys Compd. 429 (2007) 233–241.
[20] T.J. Chen, Y. Ma, B. Li, Y.D. Li, Y. Hao, Mater. Sci. Eng. A 445 (2007) 477–485.
[21] J. Blau, Walukas, Tribol. Int. 33 (2000) 573–579.
[22] A. El-Morsy, Mater. Sci. Eng. A 473 (2008) 330–335.
[23] J. An, R.G. Li, Y. Lu, C.M. Chen, Y. Xu, X. Chen, L.M. Wang, Wear 265 (2008) 97–104.
[24] K. Hiratsuka, A. Enomoto, T. Sasada, Wear 153 (1992) 361–373.
[25] N.N. Aung, W. Zhou, L.E.N. Lim, Wear 265 (2008) 780–786.
[26] J. Zhang, A.T. Alpas, Acta Mater. 45 (1997) 513–528.
[27] S. Wilson, A.T. Alpas, Wear 212 (1997) 41–49.
[28] Z. Lin, Q. Xuan-hui, D. Bo-hua, H. Xin-bo, Q. Ming-li, Trans. Nonferrous Met. Soc. China 18 (2008) 1076–1082.
[29] M. Chandrasekaran, Y.M. John, Mater. Sci. Eng. A 381 (2004) 308–319.
[30] A. El-Morsy, A. Ismail, M. Waly, Mater. Sci. Eng. A 486 (2008) 528–533.
[31] J.F. Archard, J. Appl. Phys. 24 (1953) 981–988.
[32] Y.J. Chena, Q.D. Wang, H.J. Roven, M. Karlsen, Y.D. Yu, M.P. Liu, J. Hjelen, J. Alloys Compd. 462 (2008) 192–200.
[33] H. Ding, L. Liu, S. Kamado, W. Ding, Y. Kojima, J. Alloys Compd. 456 (2008) 400–406.
[34] K. Hokkirigawa, K. Kato, Tribol. Int. 21 (1988) 51–57.
[35] C.Y.H. Lim, S.C. Lim, M. Gupta, Wear 255 (2003) 629–637.
[36] S. Das, S.V. Prasad, T.R. Ramachandran, Wear 133 (1998) 187–194.
[37] S.C. Sharma, B. Anand, M. Krishna, Wear 241 (2000) 33–40.
[38] B. Venkataraman, G. Sundararajan, Acta Mater. 44 (1996) 451–460.
[39] A.K. Mondal, B.S.S. Chandra Rao, S. Kumar, Tribol. Int. 40 (2007) 290–296.
[40] S.M. Hsu, M.C. Shen, Wear 212 (1997) 41–49.
[41] S.M. Hsu, in: B. Bhushan (Ed.), Modern Tribology Hand Book, vol. 1, CRC Press, 2001 (Chapter 9).